Supporting information

Vargo et al. 10.1073/pnas.1205426109

SI Text

SI Discussion. ***DNA coning.*** The oleosin gene was provided as a gift by Dr. Beaudoin at Rothamsted Research, Hampshire, England. PCR primers 42S (5′—AGA TAT ACC CAT ATG GCC ACC ACA ACC TAC GAC C) and 63AS (5′—TTT CTC ACC CTC GAG TTT CCC CCC TTC TTT TCG CCC TTC) were used to amplify the gene and add NdeI and XhoI restriction sites to the ends creating 42-87-63 (Oleo-WT). All genes were cloned into pBamUK, a pET series derivative, constructed in the van Duyne laboratory (SOM, Penn). pBamUK adds a 6-Histidine tag to the C terminus of the protein for IMAC purification if needed. The P = 65 family was cloned into Avi-pBamUK. A gene for a biotin binding site was created with the primers Avi S (5′—TAT GGG TCT GAA CGA CAT CTT CGA GGC TCA GAA AAT CGA ATG GCA CGA AG) and Avi AS (5′—GAT CCT TCG TGC CAT TCG ATT TTC TGA GCC TCG AAG ATG TCG TTC AGA CCC A). This gene was digested with NdeI and BamHI and ligated into pBamUK to create Avi-pBamUK. The gene for 43-65-33 was created with the primers 43S (5′—AAG GAG ATA GGA TCC TAC CGC CAT GAT CAA CAC ACC) and 33AS (5′—TAT ATG AAT CTC GAG CTG GCC CAA GTC CTT CG); 33-65-23 was created with the primers 33S (5′—AAG GAG ATA GGA TCC CTC ACC CAC CCA CAG C) and 23AS (5′—TAT ATG AAT CTC GAG ATA CTC CCC CAC ATC C); 28-65-18 was created with the primers 28S (5′—AAG GAG ATA GGA TCC CGC CAG CAA CAA GG) and 18AS (5′—AAG GAG ATA GGA TCC CGC CAG CAA CAA GG); 23-65-13 was created with the primers 23S (5′—AAG GAG ATA GGA TCC CCC TCA ACC GGC AAG ATA ATG G) and 13AS (5′—TAT ATG AAT CTC GAG CAC ATA ATC CCT CTG G). The P = 65 family was digested with BamHI and XhoI and ligated into Avi-pBamUK. All sequences were confirmed through DNA sequencing.

Protein extraction with B-PER. A 500-mL culture cell pellet was resuspended with 10 mL B-PER. DNase was added to a final concentration of 0.5 μg/mL and incubated at room temperature for 20 min. The solution was centrifuged at 15,000 *g* for 15 min and the supernatant was discarded. The resulting pellet was resuspended in 10 mL B-PER. Lysozyme was added at a final concentration of 0.2 mg/mL and incubated at room temperature for 5 min. The suspension was diluted with 25 mL of 1:10 B-PER in water and centrifuged at 15,000 *g* for 15 min and the supernatant was discarded. The resulting pellet was washed three times with 25 mL of 1:10 B-PER resulting in a purified inclusion body pellet.

Protein properties. Table S1 shows the proteins used, molecular weights, total number of amino acids, expected isoelectric points and MALDI-TOF spectroscopy peaks. The −65- set varies in molecular weight and isoelectric point. All protein variants had a 6-Histidine tag on the C terminus for potential IMAC purification.

Protein sequences. Protein mutants were created using standard PCR techniques from wild-type oleosin (42-87-63). All mutants have a 6-Histidine tag on the C terminus and the −65- family has a biotin binding tag on the N terminus for future work. Protein sequences can be found in Table S2.

Mass spectroscopy. The dual peaks observed in mass spectroscopy were due to incomplete loss of the initiation methionine (Fig. S1) (1). Expression of oleosin in inclusion bodies presumably inhibits methionine aminopeptidase from accessing the initiation methionine within the aggregated protein leading to partial removal. Expected molecular weights with and without the methionine are compared to the mass spectroscopy peaks in Table S1. In all cases, the expected protein mass with and without the methionine matches very closely with the two peaks in the MALDI-TOF spectra. No contamination peaks were observed in the spectra.

Cryo-TEM: budding. Cryo-TEM provided conclusive evidence of the morphology in solution due to the instant vitrification of the sample. Budding was observed from emulsion droplets and from bulk protein similar to polymer systems (2, 3) (Fig. S2). Therefore, it is likely that protein structures are formed due to the diffusion of chloroform through the aqueous phase creating increased protein concentrations in the emulsion forcing higher surface area structures to bud from the droplet surface (2, 3).

Cryo-TEM: membrane thickness. Vesicles appear on the micrographs as circles with a darker membrane. The inside of the vesicles will be darker compared to the bulk solution. This is due to electron scattering through the vesicle shell. The edges of the vesicles are darker due to the increased number of protein molecules that the electrons must transmit through. The membrane thickness is measured in ImageJ (4). Ten measurements were made on each vesicle and averaged to get an overall vesicle membrane thickness. Six vesicle membrane thicknesses were then averaged to get the membrane thickness for a specific mutant and plotted in Fig. 2*G*.

Fig. S3 shows representative micrographs for each point in the ionic strength phase behavior shown in Fig. 3*A*. Phases that coexisted are shown with two micrographs in the respective grid. Ice is seen as dark spherical points in a few of the micrographs and should not be misinterpreted as protein structures (Fig. S3 *C*–*E* and *H*–*K*). Fig. S3 *F*, *L*, *Q*, and *X* appear in Fig. 2 in the text. Fig. S3 *A* and *W* appear in Fig. 3 in the text.

1. Benbassat A, et al. (1987) Processing of the initiation methionine from proteins—properties of the *Escherichia-coli* methionine aminopeptidase and its gene structure. *J Bacteriol* 169:751–757.
2. Lee JCM, et al. (2001) Preparation, stability, and in vitro performance of vesicles made with diblock copolymers. *Biotechnol Bioeng* 73:135–145.
3. Zhu J, Hayward RC (2008) Hierarchically structured microparticles formed by interfacial instabilities of emulsion droplets containing amphiphilic block copolymers. *Angew Chem Int Edit Engl* 47:2113–2116.
4. Abramoff MD, Magalhaes PJ, Ram SJ (2004) Image processing with imageJ. *Biophotonics Int* 11:36–42.

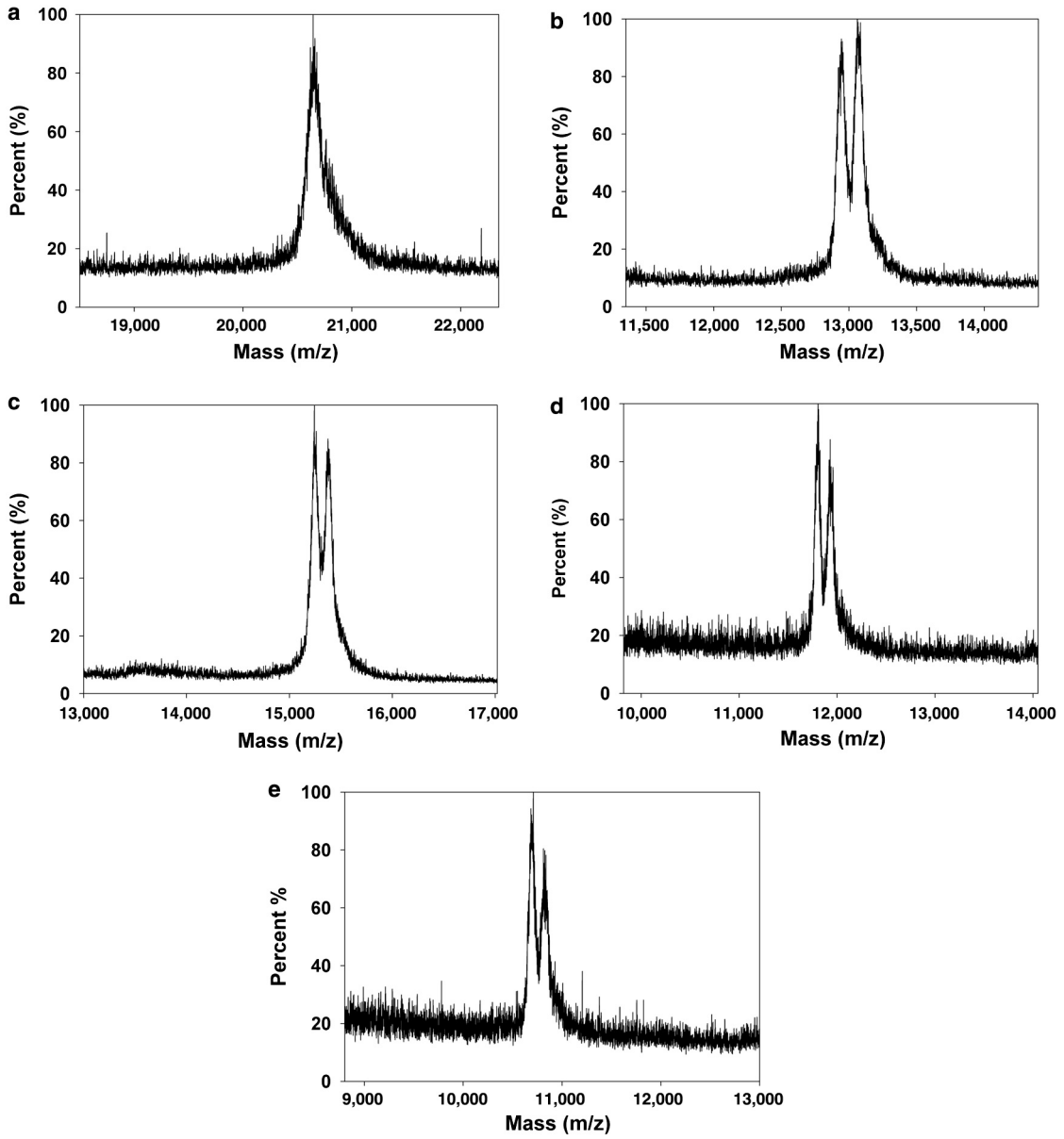

Fig. S1. (*A*–*E*) MALDI-TOF confirmed the molecular weights of the protein mutants: (*A*) 42-87-63 (wild-type oleosin), (*B*) 43-65-33, (*C*) 33-65-23, (*D*) 28-65-18, (*E*) 23-65-13. Peak closely match expected weights of the protein mutants as seen in Table S1.

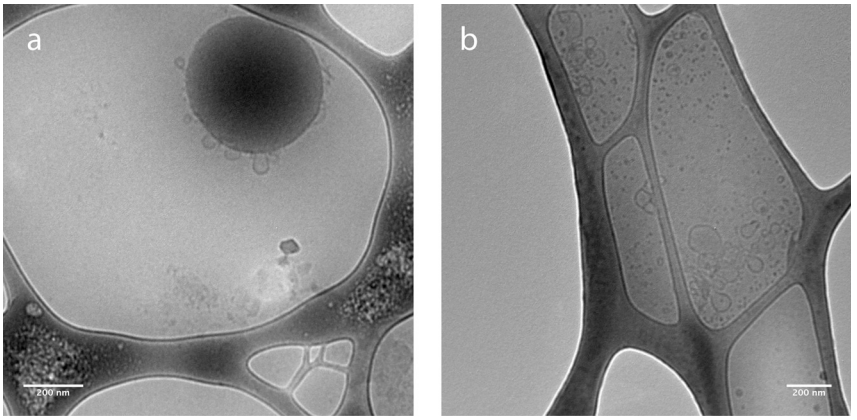

Fig. S2. Cryo-TEM micrographs of protein aggregate formation. (*A*) Cryo-TEM micrograph of 23-65-13 emulsion droplet with vesicular buds on the surface in PBS. (*B*) Cryo-TEM micrograph of 33-65-23 showing budding from dried bulk protein in PBS. Scale bars, 200 nm.

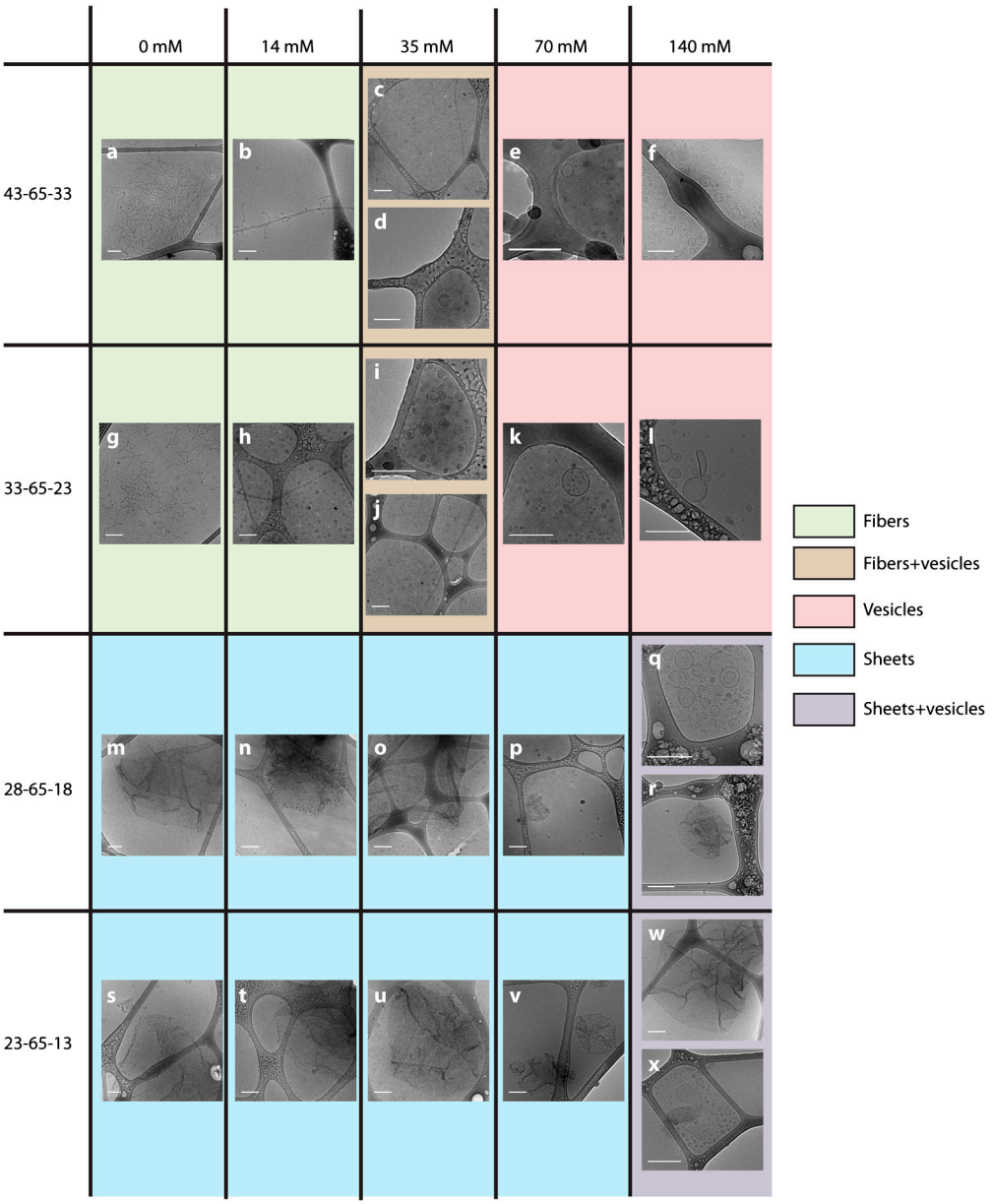

Fig. S3. Phase behavior of the −65- family in various ionic strength buffers. (*A–F*) 43-65-33 and (*G–L*) 33-65-23 shift from fibers in DI water and 14 mM ionic strength solution to fibers and vesicles in 35 mM ionic strength solution to only vesicles in 70–140 mM ionic strength solutions. (*M–R*) 28-65-18 and (*S–X*) 23-65-13 exist as sheets in 0 mM, 14 mM, 35 mM, and 70 mM ionic strength solutions and coexist as sheets and vesicles in 140 mM ionic strength solutions. Background colors match phase mapping in Fig. 4.

Table S1. Protein mutant properties and mass spectroscopy information

Protein	# Amino acids	Estimated pI	Expected MW (Da)	Expected MW (-Met) (Da)	MS peak 1 (Da)	MS peak 2 (Da)
42-87-63 (WT)	192	9.95	20,785	20,653	20,778	20,672
43-65-33	141	9.232	15,406	15,274	15,399	15,268
33-65-23	121	6.851	13,082	12,951	13,083	12,955
28-65-18	111	9.501	11,942	11,811	11,939	11,815
23-65-13	101	6.408	10,820	10,688	10,832	10,709

Table S2. Protein mutant sequences

Name	Sequence
42-87-63	MATTTYDRHHVTTTQPQYRHDQHTGDRLTHPQRQQQGPSTGKIMVIMALLPITGILFGLAGITLVGTVIGLALATPLFVIFSPVIVPA MIAIGLAVTGFLTSGTFGLTGLSSLSYLFNMVRRSTMSVPVQRDYVKGKLQDVGEYTGQKTKDLGQKIQHTAHEMGD QGQGQGQGGGKEGRKEGGKLEHHHHHH
43-65-33	MGLNDIFEAQKIEWHEGSYRHDQHTGDRLTHPQRQQQGPSTGKITGILFGLTGITLVGTVIGLALATPLFVIFSPVIVPAMI AIGLAVTGFLTSGTFGLTRSTMSVPVQRDYVKGKLQDVGEYTGQKTKDLGQLEHHHHHH
33-65-32	MGLNDIFEAQKIEWHEGSLTHPQRQQQGPSTGKITGILFGLTGITLVGTVIGLALATPLFVIFSPVIVPAMIAIGLAV TGFLTSGTFGLTRSTMSVPVQRDYVKGKLQDVGEYLEHHHHHH
28-65-28	MGLNDIFEAQKIEWHEGSRQQQGPSTGKITGILFGLTGITLVGTVIGLALATPLFVIFSPVIVPAMIAIGLAVTGFLTSGTF GLTRSTMSVPVQRDYVKGKLQLEHHHHHH
23-65-13	MGLNDIFEAQKIEWHEGSPSTGKIMGILFGLTGITLVGTVIGLALATPLFVIFSPVIVPAMIAIGLAVTGFLTSGTFGLTRSTMS VPVQRDYVLEHHHHHH